† Supplementary Information

In Vitro Assay for Single-cell Characterization of Impaired Deformability in Red Blood Cells under Recurrent Episodes of Hypoxia

Yuhao Qiang[a,b], Jia Liu[a], Ming Dao[b*], E Du[a*]

[a.] Department of Ocean and Mechanical Engineering, Florida Atlantic University, Boca Raton, FL 33431, USA.

[b.] Department of Materials Science and Engineering, Massachusetts Institute of Technology, Cambridge, MA 02139, USA.

*Correspondence should be addressed to Ming Dao (mingdao@mit.edu) and E Du (edu@fau.edu).

1. Detailed information of sickle cell samples

Table S1. Information of SCD patient samples used in the present study. HU indicates patients taking hydroxyurea.

Label	*Genotype*	*HCT*	*MCV*	*MCHC*	*WBC*	*HBS, %*	*HbF, %*	*HbA, %*	*HbA2, %*	*HbC, %*	*Reticulocytes, %*	*HU*
Patient I	HbSS	22.9	102.7	36.7	10.1	72.7	24.4	0.0	2.9	0.0	7.4	YES
Patient II	HbSS	24.4	96.1	32.4	8.74	33.7	3.0	60.4	2.9	0.0	13.6	YES
Patient III	HbSS	23.3	96.7	32.2	10.76	39.0	3.4	54.6	3.0	0.0	18.0	YES

2. Calibration of transient oxygen content in the microfluidic channel

To calibrate the transient oxygen content in the microfluidic channel for mechanical testing of individual red blood cells, we modified our microfluidic device for the convenience of the implementation of a FireStingO2 fibre-optic oxygen microsensor (Pyro Science™, Aachen, German). Fig. S1 shows the modification process with following steps:

1) The main structure of double-layer PDMS (marked by the square) was replicated from the original microfluidic device. The red arrow indicates the direction of the double-layer PDMS.

2) The double-layer PDMS was flipped and boned to a PDMS bulk with a through hole in the centre and four holes for the inlets and outlets of two microfluidic channels. All the holes were well aligned to the inter-section and inlets of the two microfluidic channels.

3) To seal the gas channel on the bottom, the whole PDMS structure was then bonded to a glass slide substrate.

4) The modified microfluidic device was placed right under oxygenation sensor, and the sensor tip was adjusted down to the cell channel through the hole in the centre.

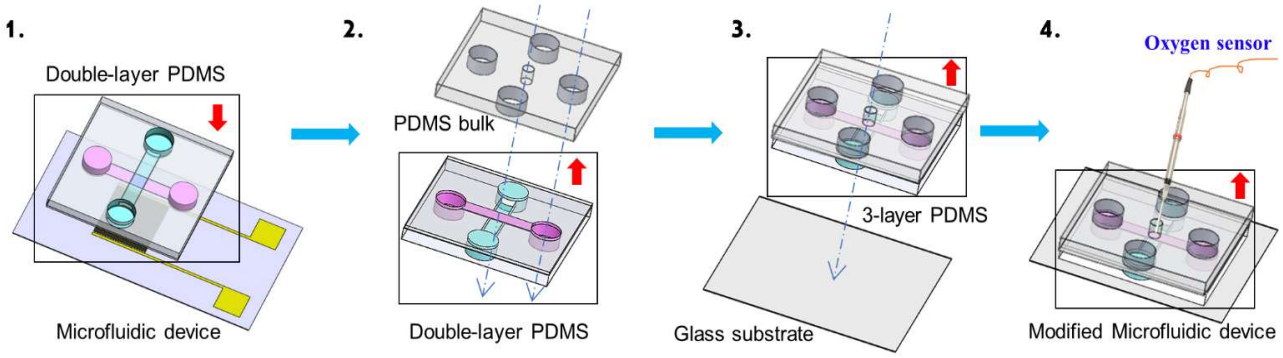

Fig. S1. Modification of microfluidic device for the calibration of transient oxygen content.

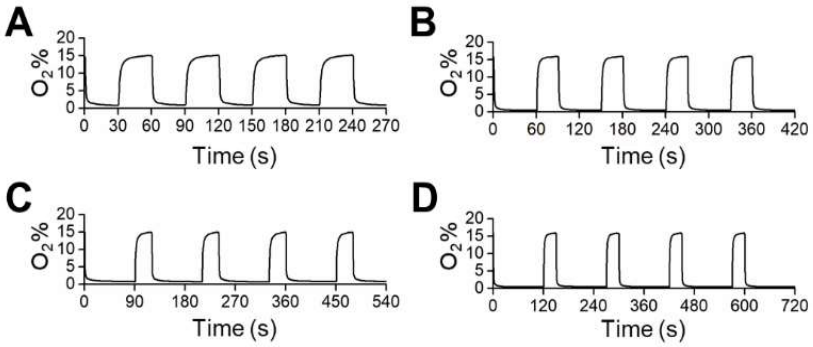

Fig. S2. Transient oxygen concentration calibrated in the cell channel under 4 different DeOxy-Oxy cycling conditions. (B) *DeOxy*(30s)–*Oxy*(30s). (C) *DeOxy*(60s)–*Oxy*(30s). (D) *DeOxy*(90s)–*Oxy*(30s). (E) *DeOxy*(120s)–*Oxy*(30s).

3. Reduction of deformability in RBCs induced by cyclic hypoxia

Table S2. Comparison of changes in the maximum extension ratio λ_{max} under different DeOxy-Oxy rate of cycling.

Accumulated DeOxy Time (min)	30s-30s	%	60s-30s	%	90s-30s	%	120s-30s	%
0	1.51 ±0.13	—	1.50 ±0.12	—	1.54 ±0.12	—	1.53 ±0.11	—
15	1.43 ±0.13	↓ 5.30	1.45 ±0.12	↓ 3.21	1.51 ±0.10	↓ 1.97	1.49 ±0.11	↓ 2.57
30	1.35 ±0.13	↓ 10.68	1.40 ±0.12	↓ 6.19	1.45 ±0.10	↓ 5.54	1.44 ±0.11	↓ 5.48

Table S3. Comparison of changes in the maximum extension ratio λ_{max} under different DeOxy-Oxy time periods.

Cycle	30s-30s	%	60s-30s	%	90s-30s	%	120s-30s	%
0	1.51 ±0.13	—	1.50 ±0.12	—	1.54 ±0.10	—	1.53 ±0.11	—
12	1.50 ±0.13	↓ 0.88	1.46 ±0.12	↓ 2.69	1.48 ±0.10	↓ 3.41	1.43 ±0.11	↓ 6.18
24	1.44 ±0.13	↓ 4.46	1.42 ±0.12	↓ 5.11	1.44 ±0.10	↓ 6.42	1.41 ±0.11	↓ 7.92

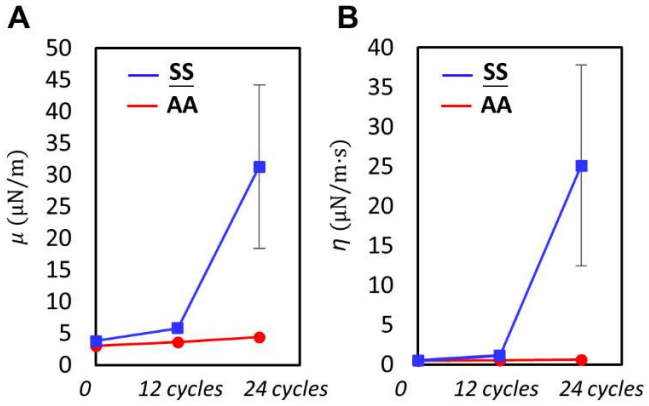

Fig. S3. Comparison of changes in the values of μ and η of normal RBCs (n=98) and identified SS RBCs (n=15) under cyclic Deoxy-Oxy (120s-30s). Data is measured at N = 0 cycle, 12 cycles and 24 cycles. SS RBCs are isolated subpopulation of sickle cells that show significant morphological changes and/or membrane crenation during the DeOxy-Oxy cycles.